Research Article

Differential effects of melatonin on adipose tissues under normoestrogenic and estrogen-deficient conditions in rats

Danielle Aparecida Munhos Hermoso[1], Lenilson da Fonseca Roza[2], Aparecida Pinto Munhos Hermoso[1], Eduardo Makiwama Klosowski[1], Franciele Neves Moreno[1], Maria Raquel Marçal Natali[3], Tatiana Carlesso dos Santos[2], Jorgete Constantin[1], Rodrigo Polimeni Constantin[1], Eduardo Hideo Gilglioni[1,4*], Emy Luiza Ishii-Iwamoto[1*]

[1]Department of Biochemistry, Laboratory of Biological Oxidation and Laboratory of Experimental Steatosis, University of Maringá, Maringá 87020900, Brazil.
[2]Department of Zootechics, University of Maringá, Maringá 87020900, Brazil.
[3]Department of Morphological Sciences, University of Maringá, Maringá 87020900, Brazil
[4] Signal Transduction and Metabolism Laboratory, Université Libre de Bruxelles, Brussels, B1070, Belgium

*Correspondence: eliiwamoto@uem.br, eduardo.hideo.gilglioni@ulb.be, Tel: 55-44-30114712

Running Title: Melatonin effects on white and brown adipose tissues in rats

Received: March 6, 2024; Accepted: August 19, 2024

ABSTRACT

In post-menopause, oxidative stress due to the decline of natural antioxidants increases the susceptibility to metabolic syndromes (MetS). Estrogen and melatonin (MEL) share antioxidant properties; however, few studies have reported the impact of estrogen deficiency and MEL treatment on morphology, redox status, and antioxidant defense capacity of diverse adipose tissue (AT) subtypes. To investigate this issue, MEL was administered to ovariectomized (OVX) rats and sham-operated rats for 16 weeks (10 mg/kg). The adipocyte morphology, oxidative stress parameters and antioxidant enzyme activity were evaluated in the visceral retroperitoneal adipose tissue (rVAT), subcutaneous inguinal adipose tissue (iSAT) and brown adipose tissue (BAT). In OVX rats, MEL treatment suppressed rVAT hypertrophy and increased the prevalence of small adipocytes in iSAT, suggesting a better lipid distribution among ATs. MEL treatment increased glutathione reductase and glucose-6-phosphate dehydrogenase activity in iSAT; therefore, restored the glutathione level. In rVAT, MEL increased glutathione peroxidase and glutathione reductase activity. MEL minimized the risks for the development of metabolic abnormalities due to estrogen deficiency. However, under normoestrogenic condition, MEL decreased plasma estradiol levels and uterine mass, raising the concerning of its effect on reproductive functions.

Key words: Melatonin**,** obesity, antioxidant, menopause, ovariectomy, oxidative stress, adipose tissue

1. INTRODUCTION

Melatonin (MEL) secreted by the pineal gland exerts chronobiotic influence on organisms (1). MEL is also synthesized by ovaries, placenta, gastrointestinal tract, immune system cells,

and retina (2-7). MEL regulates the reproductive system by modulating the hypothalamus-pituitary-gonad (HPG) axis (8) and exerting antioxidant activity in the ovarian follicles (9). Therefore, melatonin has the important roles in menopause. In addition to the climacteric symptoms, menopause is in general associated with several manifestations of metabolic syndrome (MetS), including body weight (BW) gain, type 2 diabetes, insulin resistance, nonalcoholic fatty liver disease (NAFLD), and cardiovascular diseases (10). A decline in melatonin levels in postmenopausal women has been reported in clinical studies (11, 12). Accordingly, a decreased production of MEL in metabolic disorders is supported by increased insulin resistance, glucose intolerance, and weight gain in pinealectomized rats (13). As a result, MEL emerges as a molecule for the treatment of reproductive system disorders and metabolic disturbances in women experiencing perimenopause or menopause (14-16).

MEL administration suppresses BW gain and other manifestations of MetS (16) in patients and animals with obesity and diabetes (17-19). The mechanisms underlying increased body adiposity in postmenopausal women and ovariectomized animals (OVX) are less understood compared to diet-induced obesity, but a link with estrogen deficiency has become evident, as some metabolic disorders can be reversed by estrogen therapy (20-22). Estrogens control energy homeostasis at the central (hypothalamus) and peripheral levels (23). At the central level, estrogen regulates food intake and energy expenditure (24), including the control of brown adipose tissue (BAT) thermogenesis. In peripheral tissues, predominantly the liver, pancreas, white and brown adipose tissues as well as skeletal muscle, estrogen regulates lipid metabolism, fat distribution, insulin sensitivity and thermogenesis (23).

In postmenopausal women, melatonin treatment for 1 year (1 or 3 mg nightly) reduced fat mass and increased lean mass, without significant changes in body weight and blood levels of leptin, insulin, or markers of glucose homeostasis (25). Research conducted in OVX rodents, in which different routes, doses, and duration of melatonin treatment were used, has demonstrated the capacity of MEL to ameliorate alterations in body weight and adiposity (21, 26, 27), dyslipidemia and insulin resistance (21, 27) and hepatic steatosis (26, 28). It appears that the action of MEL under estrogen deficiency is not related to the regulation of feeding behavior, as food intake and serum levels of leptin or adiponectin were not altered by MEL (26-28). An increase in energy expenditure and a decrease in hepatic lipogenesis have been suggested by Hsu and Chien (26), as MEL promotes the browning of white adipose tissues through irisin and a decrease in the RNA levels of hepatic fatty acid synthesis enzymes. In our previous study with ovariectomized (OVX) rats we demonstrated that the administration of MEL, beginning 13 weeks after ovariectomy and continuing for 3 weeks, reversed hepatic steatosis and oxidative damage (28). However, we have not found suppression of BW gain or abdominal fat accumulation.

It is known that regardless of the whole-body adipose tissue (AT) gain, the regional deposition of AT and adipose morphology are the more precise predictors of the risks for metabolic disturbances associated with obesity (29-33). Hyperplasia of adiposity (the formation of new adipocytes) is considered healthy and adaptive. However, excessive lipid overload and a massive expansion of existing adipocyte cells (hypertrophy), is associated with oxidative stress, inflammation, necrosis, and ectopic lipid deposition (29-31, 34). A study in postmenopausal women showed more visceral adipose tissue (VAT) and subcutaneous adipose tissue (SAT) than premenopausal women, and considerable differences in SAT and VAT phenotype, i.e., increased SAT inflammation was associated with the accumulation of VAT and the change in VAT morphology was related to insulin resistance (35). It has been suggested that the differential expression of estrogen receptors (ERs) *ER1* and *ER2* in VAT and SAT is related to adipocyte functions such as glucose uptake and insulin sensitivity (36).

Reactive oxygen species (ROS) are important signals for proper adipogenesis (37). However, lipid overload can lead to excessive generation of ROS, an early event in the

adipocyte dysfunction (37, 38). In postmenopausal women, oxidative stress due to the decline of estrogens plays a critical role in the susceptibility to MetS and insulin resistance level, a condition that may be related to the loss of the antioxidant action of estrogens (39, 40). The anti-obesity effect of estrogen involves multiple mechanisms, including its direct action as a ROS scavenger, a reaction linked to its ring A hydroxyl group (41), and also by positively regulating the expression of antioxidant genes through estrogen receptor signaling (42, 43). However, little is known about how estrogen deficiency affects the morphology, redox state, and capacity of the antioxidant defense system of the adipocytes in the different subtypes of fat deposits between visceral and subcutaneous white adipose tissue (WAT) and brown adipose tissue (BAT). MEL and estrogen share a buffering capacity to scavenge oxygen and nitrogen reactive species (ROS/RNS) and to activate antioxidant defense systems (44-46). It has not yet been determined whether the actions of MEL in females under estrogen-deficiency or normoestrogenic conditions involve changes in the relative weights of VAT, SAT and BAT, and in the adipocyte phenotype in these ATs.

To examine the therapeutic potential of MEL in correcting adipose tissue dysfunction, MEL was administered orally to OVX and sham-operated (CON) rats, starting on the day of surgery and continuing for 16 weeks. The relative contribution of subcutaneous and visceral WAT and BAT to body adiposity, the morphology, the redox state, and the antioxidant defense capacity of each of these ATs were evaluated.

2. MATERIALS AND METHODS

2.1. Chemicals.

N-acetyl-5-methoxytryptamine (MEL), adenosine diphosphate (ADP), 2,4-dinitrophenol (2,4-DNP), phenylmethylsulfonyl fluoride (PMSF), oxidized glutathione (GSSG), reduced glutathione (GSH), sodium dodecyl sulfate (SDS), o-phthalaldehyde (OPT), 2',7'-dichlorofluorescein diacetate (DCFH-DA), 2',7'-dichlorofluorescein (DCF), 5,5'-dithiobis (2-nitrobenzoic acid) DTNB, β-nicotinamide adenine dinucleotide phosphate, reduced dipotassium salt (NAD[P]H), pirogallol and enzymes used in analytical methods were from Sigma Chemical Co. (St. Louis, USA). Kits from Gold Analisa® (Belo Horizonte, Brazil) were used to measure blood lipids and glucose levels. Sodium heparin was obtained from Roche (São Paulo, Brazil).

2.2. Animals.

The female Wistar rats weighing 130–160 g (6 weeks) were supplied by Central Biotery of the University of Maringá and were randomly assigned to a sham operation (CON) or a bilateral ovariectomy (OVX) groups. They were kept in the sectorial Laboratory of the Department of Biochemistry, with a controlled temperature of 25 °C and a light/dark cycle of 12/12 hours. The light was turned on at 6 AM and turned off at 6 PM. The rats were housed in the polypropylene cages (a maximum of four animals per cage) and they accessed to standard diet and water *ad libitum*. After acclimatization, the animals were anesthetized with xylazine (10 mg/kg) + ketamine (50 mg/kg) to bilateral ovariectomy surgery. The CON rats were subjected to the same procedures as the OVX rats, but their ovaries were exposed without being removed. The surgeries were performed in the morning (7:00 to 9:00 AM, representing ZT 1 to ZT 3). All experiments were conducted in strict adherence to the guidelines of the Ethics Committee for Animal Experimentation of the University of Maringá (CEUA no. 6631250815).

2.3. Animal treatment and sample collection.

The rats were divided into four groups: sham-operated as the control (CON); ovariectomized (OVX); CON with MEL (CON+MEL); and OVX with MEL (OVX+MEL). The day after surgery, a dose of 10 mg/kg of MEL dissolved in 0.9% saline solution was administered every morning (8:00 AM) to CON+MEL and OVX+MEL rats by gavage (final volume of 400 µL) over a period of 16 weeks. The rats in the CON and OVX groups received the same volume of 0.9% saline solution. Food intake and BW were recorded every two days throughout the trial period. On the final day of the study, the overnight-fasted animals were anesthetized with thiopental sodium (50 mg/kg *i.p.*) and the blood, uterus, the retroperitoneal, uterine, mesenteric and inguinal WAT as well as interscapular BAT were collected. These procedures were carried out between 07:00 AM (ZT 1) and 09:00 AM (ZT 3). The retroperitoneal, uterine, mesenteric and inguinal WATs were weighed, and the adiposity index was calculated as the ratio of the weights (in grams) of these WATs per 100 g of BW (47).

Blood was collected by cardiac puncture to obtain serum to measure serum estradiol. The blood was collected at 7:00 AM (ZT 1) from female rats on the first day of the estrous cycle; the other assays were performed in randomly cyclic females.

2.4. Measurement of carcass composition.

The contents of the dry matter (DM), crude protein (CP), ether extract (EE), and mineral matter (MM) were measured in the frozen carcasses (n = 6 per treatment) that were milled in an industrial meat mill with hair, viscera, feet, and heads (48). The samples were homogenized, and an aliquot of 60 g was lyophilized for 36 hours for the determination of DM. For the determination of MM, aliquots of lyophilized samples were weighed in porcelain crucibles, oven-dried at 105 °C for 24 hours, transferred to a muffle at 550 °C, and incinerated to determine the ash value. CP was obtained using the Kjeldahl nitrogen method (CP = nitrogen x 6.25). EE was obtained by extraction in a Soxhlet extractor.

2.5. Biochemical analysis of serum.

Estradiol was determined by chemiluminescence method in the Laboratório Veterinário São Camilo, Maringá. The estrous cycle of the rats was evaluated by the vaginal smear technique by instilling 0.3 ml of saline (0.9% NaCl), and the vaginal aspirate was collected. The fresh, uncolored slides were examined for the differentiation of the cell types (epithelial cells, cornified cells, and leukocytes). When the proestrus phase, a stage with the highest prevalence of epithelial cells (49, 50) was identified, the blood was collected the next day for analysis.

Glucose, triglycerides, total cholesterol, and high-density lipoprotein (HDL) were analyzed in serum using assay kits (Gold Analisa®) following the manufacture's instructions. Very-low-density lipoprotein (VLDL) levels were calculated using the Friedewald equation (51), and low-density lipoprotein (LDL) levels were determined by subtracting HDL and VLDL from total cholesterol. The hepatic aspartate aminotransferase (AST) and alanine aminotransferase (ALT) were analyzed in plasma samples using standard assay kits (Gold Analisa®) following the manufacture's instructions. The results were expressed as international units (IU) per liter

2.6. Histological and histochemical analysis of ATs.

Samples from retroperitoneal visceral adipose tissue (rVAT), inguinal subcutaneous adipose tissue (iSAT), and BAT (n = 3–6 per treatment) were fixed in Carnoy's solution (60% absolute ethanol, 30% chloroform, and 10% acetic acid) and embedded in histological paraffin

(BIOTEC®, Pinhais, PR, Brazil). Nonserial histological sections (5 µm thick) were obtained using a Leica RM2145 semi-motorized rotary microtome (Leica Biosystems, Richmond, USA) and stained with hematoxylin and eosin (H&E). Images were captured with 20× and 40× objectives (25 to 50 images per animal) with an Olympus BX41 light microscope equipped with an Olympus Q-Color 3 camera and a microcomputer (Q-Capture software).

The morphometric analyses of rWAT and iSAT were performed using captured digital images (TIFF 24-bit color, 2560 x 1920 pixels), and the adipocyte area of 1,200 cells per group from 4–6 rats for each experimental group was measured and analyzed with the Image-Pro Plus 4.5 software (Media Cybernetics, Silver Spring, MD, USA). Any objects that fell below an area of 350 μm^2 were removed, and the distribution from 0 to 15,000 μm^2 in 500 μm^2 increments was appropriate for most AT depots. The number of total adipocytes within the distribution was calculated and used to convert the frequency to a percentage of the total adipocytes counted. The area occupied by the vacuoles (lipid droplets) in the samples of BAT stained with H&E was related to the total area (area of lipid droplets in % of µm × 100^{-1} × total area of the $image^{-1}$).

2.7. Determination of malondialdehyde, thiol, and GSH content in ATs.

The lipid peroxidation level was evaluated in samples of the rVAT, iSAT, and BAT from overnight-fasted rats by detection of thiobarbituric acid-reactive substances (TBARS), predominantly malondialdehyde (MDA). Samples of each AT were clamped in liquid nitrogen and homogenized in a medium containing 250 mM sucrose, 1 mM ethylene glycol-bis (2-aminoethyl ether)-*N*,*N*,*N*',*N*'-tetraacetic acid (EGTA), and 10 mM 4-(2-hydroxyethyl)-1-piperazineethanesulfonic acid (HEPES; pH 7.2) in the proportions of 1g/4mL (liver), 1g/2mL (rVAT and iSAT), and 1g/3mL (BAT). Aliquots of total homogenates (0.2 to 0.6 mg of protein) were added to 4 mL of a solution containing 0.4% SDS, 7.5% acetic acid, and 0.25% thiobarbituric acid (TBA). After 1 hour of incubation at 95 °C, the MDA-TBA complex was extracted with 4 mL of n-butanol/pyridine 15:1 (v/v), and the absorbance was determined at 532 nm ($\varepsilon = 1.56 \times 10^5$ M^{-1} cm^{-1}). The lipoperoxide level was calculated from the standard curve of 1,1,3,3-tetraethoxypropane, and the values were expressed as nmol (mg of $protein^{-1}$) (52).

For the determination of protein thiol content, samples of ATs clamped in liquid nitrogen were homogenized in a medium containing 0.02 mol/L ethylenediaminetetraacetic acid (EDTA; pH 8.2) in the proportions of 1g/2 mL (rVAT and iSAT) and 1g/3 mL (BAT). Aliquots of total homogenates (1.0 to 1.5 mg of proteins) were added to 0.2 mL of a medium containing 15% trichloroacetic acid. The mixture was centrifuged at 9.500 × *g* for 10 min, and the supernatant was suspended in a medium containing 0.1 M NaH_2PO_4, 5 mM EDTA, and 10 mM DTNB [53]. After 15 min in the dark at room temperature, the absorbance was determined at 412 nm. The protein thiol content was calculated using the ε value of 1.36×10^4 M^{-1} cm^{-1} and expressed as nmol $(mg\ of\ protein)^{-1}$.

For the measurements of GSH, aliquots of the total homogenates of ATs (1.0 mg of protein), prepared as described for MDA determination, were diluted in 1.5 mL of a medium containing 125 mM sucrose, 65 mM KCl, 10 mM HEPES (pH 7.4), and 15% trichloroacetic acid. After centrifugation at 10,000 × *g* for 3 min, the supernatant was used for GSH measurement using OPT (54). The samples (100 µL) were added to 2.0 mL of a medium containing 0.1 M phosphate buffer (pH 8.0) and 5.0 mM EDTA. The reaction was started by adding 100 µL of OPT solution (1 mg/mL in methanol). The fluorescent product GSH-OPT was measured fluorometrically (350 nm excitation and 420 nm emission) after incubation for 15 min at room temperature. The results were expressed as µg GSH $(mg\ of\ protein)^{-1}$.

2.8. Determination of antioxidant enzyme activities in ATs.

The activities of superoxide dismutase (SOD), glutathione peroxidase (GPx), and glutathione reductase (GR) were measured in a soluble cytosolic fraction of ATs. Samples of 3.0 g (rVAT and iSAT) or 2.0 g (BAT) were homogenized in an ice-cold medium containing 5 mL of potassium phosphate 0.1 M (pH 7.4) using a Dounce homogenizer. After centrifugation at 15,000 × g for 10 min, the supernatants were collected for enzyme measurement.

The SOD activity was estimated by its capacity to inhibit pyrogallol autoxidation (55). Aliquots of supernatant equivalent to 0.3 mg of protein from iSAT, 0.2 mg of protein from rVAT, and 0.4 mg of protein from BAT were added to 1000 µL of a medium containing 200 mM Tris-HCl buffer (pH 8.2), 2 mM EDTA, and 70µL of 1.05 mM pyrogallol. After 3 min of reaction, the absorbance was measured at 420 nm. The number of enzymes sufficient to inhibit the pyrogallol autoxidation by 50% (IC_{50}) was defined as 1 unit of SOD. The results were expressed as U (mg of protein)$^{-1}$.

GPx activity was assessed using H_2O_2 as a substrate in the presence of nicotinamide adenine dinucleotide phosphate (NADPH) and GSH (56). Aliquots of supernatant equivalent to 0.3 mg of protein from iSAT, 0.1 mg of protein from rVAT, and 0.2 mg of protein from BAT were added to 1.5 mL of a medium containing 350 µL of 171 mM potassium phosphate (pH 7.0), 4.28 mM sodium azide, and 2.14 mM EDTA. The reaction was initiated by adding a mixture containing 250 µL of 1.5 mM GSH, 300 µL of 0.27 mM NADPH, 10 µL of 2 U/mL GR, 520 µL of double-distilled H_2O, and 30 µL of 0.18 mM H_2O_2. The enzymatic reaction was monitored by the decrease in NADPH absorbance for 90 seconds at 340 nm. The initial rate (15 s) was extrapolated to calculate the enzymatic activity using the molar extinction coefficient (ε) of NADPH (6.220 M^{-1} cm^{-1}). The enzymatic activity was expressed as nmol of NADPH oxidized (min×mg of protein)$^{-1}$.

The decrease in NADPH absorbance at 340 nm in the presence of oxidized glutathione (GSSG) was used for determining GR activity (57). Aliquots of supernatant equivalent to 0.2 mg of protein from iSAT or 0.1 mg of protein from BAT and rVAT were incubated in a medium containing 850 µL of 50 mM K_2HPO_4 buffer (pH 8.0) and 1.8 mM EDTA. The reaction was initiated by adding 50 µL of 0.5 mM GSSG and 50 µL of 0.15 mM NADPH, and the decrease in absorbance was followed for 90 s at 340 nm. The initial rate (15 s) was extrapolated to calculate the enzymatic activity using the ε of NADPH (6.220 M^{-1} cm^{-1}). The enzymatic activity was expressed as nmol of NADPH reduced/min×mg of protein.

For the measurements of catalase (CAT) activity, approximately 1.0 g of rVAT, iSAT, and BAT removed from overnight-fasted rats were clamped in liquid nitrogen and homogenized in a medium containing 0.1 M potassium phosphate (pH 7.4). After centrifugation at 15,000 × *g* for 10 min, the supernatant was collected. The enzyme reaction was initiated by the addition of aliquots of supernatant equivalent to 0.04 mg of protein from rVAT, 0.06 mg of protein from iSAT, or 0.08 mg of protein from BAT in 1.0 mL of a reaction medium containing 1.0 M Tris (pH 8.0) + 50 mM EDTA, 0.02% of Triton X-100, and 25.2 mM of H_2O_2. The change in absorbance due to H_2O_2 consumption was followed at 240 nm. The enzymatic activity was expressed as H_2O_2 consumed (min×mg of protein)$^{-1}$, using the ε of H_2O_2 (33.33 M^{-1} cm^{-1}) (58).

For measurements of glucose-6-phosphate dehydrogenase (G6PD) activity, a sample of 3.0 g (rVAT and iSAT) or 2.0 g of BAT was homogenized in 5 mL of potassium phosphate 0.1 M (pH 7.4). The homogenates were centrifuged at 30,000 × *g* for 15 min, and the supernatant was collected. The supernatants were added to 1 mL of reaction medium containing 50 mM Tris (pH 8.1), 1.0 mM MgCl, 0.1 mM $NADP^+$, and 0.2 mM glucose-6-phosphate. After incubation for 5 min at 37 ºC, the enzymatic activity was estimated by the rate of absorbance increase at

340 nm due to $NADP^+$ reduction (59). The enzymatic activity was expressed as nmol of NADPH (min×mg of protein)$^{-1}$ using the ε of NADPH (6.220 $M^{-1}cm^{-1}$).

2.9. Statistical analysis.

The data were expressed as mean ± standard errors (SE). Normal distribution was tested by Shapiro–Wilk test. Data were analyzed by two-way ANOVA with animal condition (SHAM x OVX) and treatment (Saline x MEL) as factors. Pairwise comparisons of significant main effects or interactions were made using Tukey's Honestly Significant Difference (HSD) test ($p \leq 0.05$). When homogeneity of variance was not met, data were analyzed by a one-way non-parametric ANOVA followed by the Kruskal-Wallis test. The statistical analysis was performed with the Prism GraphPad software (GraphPad Software, Inc.). $p < 0.05$ was considered statistically significant.

3. RESULTS

3.1. The effects of treatments on BW gain, food consumption, and body carcass composition.

The BW of rats in four groups increased progressively during the 16 weeks of treatment (Fig. 1A). After 10 weeks of treatment, the BW of OVX rats was higher than that of CON rats, reaching a higher value at the end of the experimental period, corresponding to an increment of 8.8% in the area under the curve of BW. MEL administration to OVX rats (OVX+MEL) did not modify the pattern of BW gain compared to untreated OVX rats, and the area under the BW curve remained 12.1% higher than that of CON rats at week 16. Contrasting with this lack of effect on OVX rats, MEL reduced the BW gain of CON rats after 12 weeks of the treatment, reaching a reduction of 8.9% in the area under the BW curve (Figure 1A). Despite the fact that OVX and OVX+MEL rats had a higher BW gain than the CON rats, the cumulative and mean weekly energy intake was not different among them (Fig.1B). In CON+MEL rats, the lower body weight gain was associated with a reduction in cumulative energy intake after 14 weeks, reaching a 21% lower value compared to the CON rats at the end of the experimental period. However, the mean weekly energy intake over the whole period was not different among CON and CON+MEL rats (Figure1B).

The success of the ovariectomy surgery was confirmed by a 75% decrease of serum estradiol level in OVX rats compared to CON rats (Table 1). Under control conditions (CON+MEL), MEL induced a 53% reduction in estradiol levels compared to CON rats. No significant differences were observed among the four groups as to the blood levels of glucose, triglycerides, total cholesterol, and lipoproteins. The activities of AST and ALT were modified in OVX rats, which increased by 46% and 28%, respectively, compared to the CON rats. MEL treatment partially reversed the levels of both enzymes in OVX+MEL rats but did not alter the enzymes in CON+MEL rats compared to their respective untreated rats.

Figure 2 listed the composition of the whole-body carcasses of the rats relative to their contents of the total humidity to dry matter (DM, panel A), mineral matter (MM, panel B), crude protein (CP, panel C), and ether extract (EE, panel D). Total humidity was 5% lower in OVX rats compared to the CON rats, and MEL treatment did not modify this parameter in either the CON+MEL rats or the OVX+MEL rats (Figure 2A). No significant differences were found in the percentage of MM among the four groups (Figure 2B).

The percentage of CP did not differ between CON and OVX rats (Figure 2C), and MEL treatment increased by 5% the CP in CON+MEL rats compared to the CON group but without changes in OVX+MEL rats. The most significant difference between groups was the

percentage of EE (Figure 2D). OVX rats exhibited a 13% increase in EE relative to values in CON rats, and this parameter remained elevated in OVX+MEL rats (+21% relative to CON rats). However, MEL induced a decrease of 18% in the percentage of EE in CON+MEL rats. These results indicated that the corporal lipid accounted for the majority of the BW gain differences between groups (Figure 1A). We then examined the weights of different AT depots including uterine visceral adipose tissue (uVAT), mesenteric visceral adipose tissue (mVAT), rVAT, and iSAT.

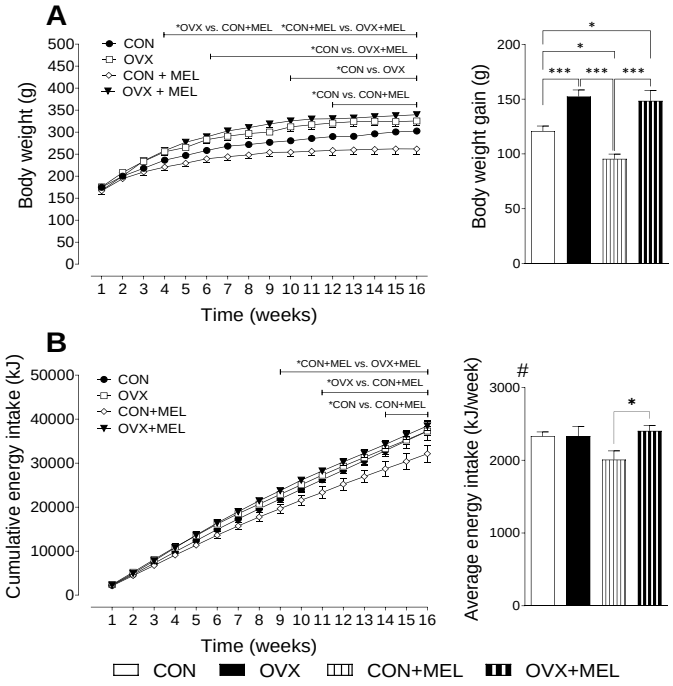

Fig. 1. Effects of OVX and MEL on biometrical parameters of rats.

*A. The body weight (BW) and the area under the curve of BW gain (n = 8). B. Weekly cumulative energy intake and the average energy intake per week (n = 8 per group). MEL: melatonin, CON: sham-operated rats, OVX: ovariectomized rats, CON+MEL: MEL-treated control rats, and OVX+MEL: MEL-treated OVX rats: The values are the mean ± SE. The significant differences were evaluated using a two-way analysis of variance (ANOVA) with Tukey's post-hoc test: * p ≤0.05; **p ≤0.01; ***p ≤0.001. #: Significant main effect of animal condition (SHAM x OVX); &: Significant main effect of treatment (Saline x MEL).*

Table 1. Effects of OVX and MEL on biochemical parameters of blood.

	CON	OVX	CON+MEL	OVX+MEL
Estradiol ╪#	32.67 ± 10.66	8.00 ± 1.63[a]	14.00± 2.16[b]	15.33 ± 4.92[c]
Glucose	90.99 ± 4.39	90.49 ± 3.81	76.65 ± 4.57	87.06 ± 5.78
Triglyceride	31.73 ± .290	33.70 ± 2.57	31.73 ± 4.88	34.36 ± 2.77
Total cholesterol	66.94 ± 4.42	70.66 ± 2.21	64.84 ± 6.09	63.83 ± 5.53
HDL-cholesterol	31.78 ± 2.53	30.66 ± 2.23	22.63 ± 2.82	26.13 ± 3.35
LDL-cholesterol	31.27 ± 2.32	33.30 ± 2.21	37.98 ± 2.96	32.45 ± 2.39
VLDL-cholesterol	5.908 ± 0.42	6.383 ± 0.40	5.738 ± 0.37	6.440 ± 0.42
AST ╪#	59.45 ± 3.22	86.68 ± 4.52[a]	69.63 ± 3.94	72.92 ± 4.10[d]
ALT ╪	28.79 ± 2.20	36.76 ± 2.01[a]	32.21 ± 2.86	26.04 ± 1.10[d]

MEL: melatonin, CON: sham-operated rats, OVX: ovariectomized rats, CON+MEL: MEL-treated control rats, OVX+MEL: MEL-treated OVX rats. The unit of estradiol was expressed as pg/mL. The units of glucose, triglyceride, total cholesterol, high-density lipoprotein (HDL) cholesterol, low-density lipoprotein (LDL) cholesterol, very-low-density lipoprotein (VLDL)

cholesterol were expressed as mg/dL, and AST and ALT were expressed as U/L. Values are expressed as the mean ± standard error (SE) of 4–14 animals per group. The letters indicate the statistical significance as revealed by a two-way analysis of variance (ANOVA) followed by a Tukey post-test ($p < 0.05$): [a]OVX vs. CON; [b]CON vs. CON+MEL; [c]CON vs. OVX+MEL; [d]OVX vs. OVX+MEL. #: Significant main effect of animal condition (SHAM x OVX); ╪: Significant interaction between animal condition (SHAM x OVX) and treatment (Saline x MEL).

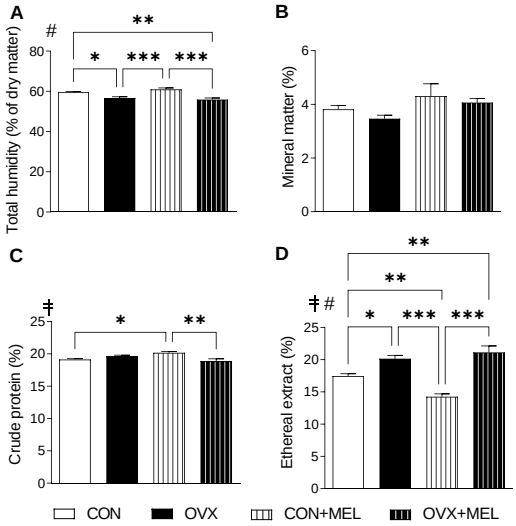

Fig. 2. Effects of OVX and MEL on carcass composition.

*A. total humidity % of DM (n = 6). B. mineral matter (MM, n = 6). C. crude protein (CP, n = 6). D. ethereal extract (EE, n = 6). The values are the mean ± SE. MEL: melatonin, CON: sham-operated rats, OVX: ovariectomized rats, CON+MEL: MEL-treated control rats, OVX+MEL: MEL-treated OVX rats. The significant differences between the values were evaluated using a two-way analysis of variance (ANOVA) with Tukey's post-hoc test: * $p \leq 0.05$; ** $p \leq 0.01$; *** $p \leq 0.001$. # = Significant main effect of animal condition (SHAM x OVX); ╪ = Significant interaction between animal condition (SHAM x OVX) and treatment (Saline x MEL).*

3.2. Effects of OVX and MEL on adiposity index and the weights of uterine retroperitoneal, mesenteric, and inguinal fats.

The adiposity index, calculated as the sum of the rVAT, mVAT, uVAT, and iSAT fat weights relative to 100 g of BW (Figure 3A), revealed 17% higher adiposity in OVX rats compared to CON rats, a value that remained elevated (18%) in MEL-treated rats (OVX+MEL). These results are in accordance with those found in the percentage of corporal EE (Figure 2D). Such a correlation was not found in the CON+MEL rats, as the adiposity index was not reduced by MEL treatment. The ovariectomy and/or MEL treatment exerted a distinct influence on the weights of each AT: the weights of uVAT (Figure 3B) and rVAT (Figure 3C) were not affected by both ovariectomy and MEL treatments; the weight of iSAT in OVX rats was 86% higher than that of the CON rats (Figure 3E), and MEL administration (OVX+MEL) did not suppress this effect. The weight of mVAT was not different among OVX and CON rats, but MEL reduced the weight in CON+MEL rats (–25%) without alteration in OVX+MEL rats compared to their respective untreated rats (Figure 3D).

Figure 3 also shows the influence of ovariectomy and MEL treatment on uterine weight (Figure 3F). As expected, pronounced uterine atrophy was observed in OVX rats, with a reduction of 85% in uterus weight compared to that of CON rats. This effect was not affected

by the MEL administration. However, MEL reduced by 17% the weight of the uterus in CON+MEL rats compared to the values in CON rats.

For the next assays, three representative ATs were selected: the retroperitoneal visceral adipose tissue (rVAT), inguinal subcutaneous adipose tissue (iSAT), and interscapular BAT.

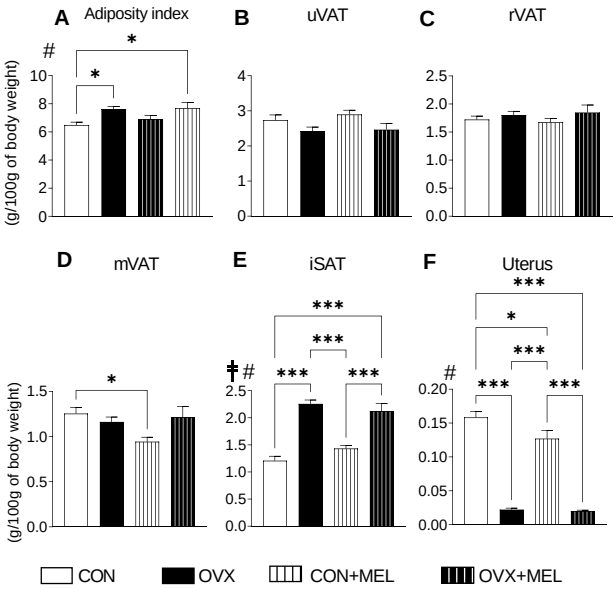

Fig. 3. Effects of OVX and MEL on adiposity index and the weights of uterine retroperitoneal, mesenteric, inguinal fats and uterus weight at the end of treatment (16 weeks).

*A. adiposity index calculated from the sum of the retroperitoneal visceral adipose tissue (rVAT), uterine (uVAT), mesenteric (mVAT), and inguinal subcutaneous adipose tissue (iSAT) weights (n = 6–10). B. uVAT weight (n = 8–11). C. rVAT weight (n = 6–8). D. mVAT weight (n = 8–9). E. iSAT weight (n = 6–9). F. uterusu weight (n = 8–11). MEL: melatonin, CON: sham-operated rats, OVX: ovariectomized rats, CON+MEL: MEL-treated control rats, OVX+MEL: MEL-treated OVX rats. All the weights were expressed in g/100 body weight (BW). The values are the mean ± SE. The significant differences were evaluated using a two-way analysis of variance (ANOVA) with Tukey's post-hoc test: * $p \leq 0.05$; ** $p \leq 0.01$; *** $p \leq 0.001$. #: Significant main effect of animal condition (SHAM x OVX); ╪: Significant interaction between animal condition (SHAM x OVX) and treatment (Saline x MEL).*

3.3. Effects of OVX and MEL on morphometric parameters of ATs.

Figure 4 (panels A to L) shows representative histological images of rVAT and iSAT from the four groups of animals. Despite the lack of alteration in rVAT weight by ovariectomy or MEL treatment (Figure 3C), the images of the rVAT revealed larger adipocytes (Figure 4B) in OVX rats compared to those of CON rats (Figure 4A). The mean area of adipocytes in rVAT, which was 2736 ± 177 in CON rats, increased to 3681 ± 352 (+35 %; $p = 0.05$) in OVX rats. These findings were confirmed by analysis of the distribution of adipocytes according to their areas. The curve of the frequency of adipocytes in OVX (Figure 3F) rats was shifted toward the right side relative to the CON curve (Figure 3E), corresponding to adipocytes with larger areas. In CON rats, the higher frequency of adipocyte sizes was between 501 and 2000 μm^2, whereas in OVX rats, it was between 2001 and 3500 μm^2.

MEL administration did not modify the frequency curve of CON+MEL rats compared to the CON rats (Figures 4 G). However, significant changes were found in OVX rats (Figure 4H), with their frequency curve approaching that of the CON curve. This occurs due to a

substantial increase in the frequency of adipocytes from 501 to 2000 μm^2 and a decrease in the frequency of adipocytes in areas between 3501 and 5000 μm^2. The mean area of adipocytes in CON+MEL (2428 ± 136 μm^2) and OVX+MEL (2787 ± 1439 μm^2) did not reveal statistical differences from their respective untreated controls.

Different features were found in iSAT. Although the iSAT weight in OVX rats practically doubled relative to CON rats (Figure 3E), the histological image revealed that the adipocyte sizes did not differ significantly between these groups (Figures 4I, J). The mean area of adipocytes in iVAT was 2808 ± 108 μm^2 in CON rats and 2517 ± 266 μm^2 in OVX rats. In addition, no differences were found in the curve of frequency of adipocytes in any range of adipocyte sizes (Figures 4 M, N). The MEL treatment induced significant changes in the two groups of rats, increasing the frequency of small adipocytes. This effect was more accentuated in CON+MEL rats, whose mean adipocyte area decreased to 1700 ± 74 μm^2 compared to CON rats (–40%; p = 0.0012). Despite no significant difference in the mean adipocyte area in OVX+MEL (2023 ± 98 μm2) and OVX rats (2517 ± 267 μm2), the curve of frequency of adipocytes revealed a significant increase in the proportion of small adipocytes (501–2000 μm^2) in OVX+MEL rats (Figure 4P), as it was also found in CON+MEL rats (Figure 4O) relative to their untreated control rats.

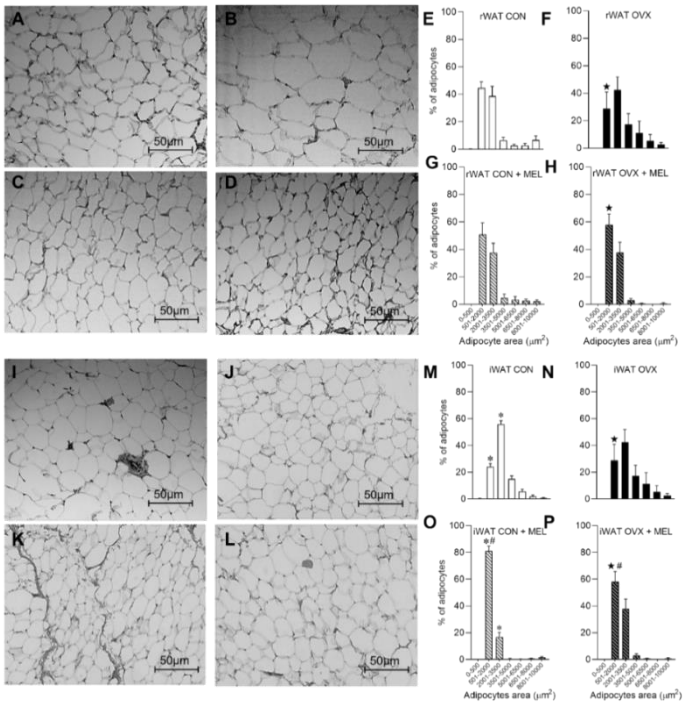

Fig. 4. Effects of CVX and MEL on histological and morphometric parameters of adipose tissues (ATs).

*ATs were stained with H&E and adipocyte area quantification expressed as the percentage of total cells quantified. A, E. The retroperitoneal visceral adipose tissue (rVAT) from CON. B, F. The rVAT from OVX; (C, G) The rVAT from CON+MEL. D, H. The rVAT from OVX+MEL. I, M. The inguinal subcutaneous adipose tissue (iSAT) from CON. J, N. The iSAT from OVX. K, O. The iSAT from CON+MEL. L, P. The iSAT from OVX+MEL. MEL: melatonin, CON: sham-operated rats, OVX: ovariectomized rats, CON+MEL: MEL-treated control rats, OVX+MEL: MEL-treated OVX rats. All data are expressed as the mean ± SE of 4–5 individual experiments. The significant differences were evaluated using a two-way analysis of variance (ANOVA) with Tukey's post-hoc test. Bars marked with the same symbols indicate signifcant differences (p < 0.05) between the following pairs: *CON vs. CON+MEL; ★OVX vs. OVX+MEL; # CON+MEL vs. OVX+MEL.*

In addition to WAT, the representative histological images of BAT obtained with the soluble dye of H&E (Figure 5) revealed that OVX (Figure 5B) and OVX+MEL (Figure 5D) rats had more vesicles, likely lipid inclusions, than that of CON rats (Figure 5A). The quantitative morphometric analysis (Figure 5E) revealed that the area occupied by these vesicles in OVX rats was 35% higher than in that in CON rats, and MEL treatment (OVX+MEL) did not modify this parameter. No significant difference was found in CON+MEL rats compared to CON rats.

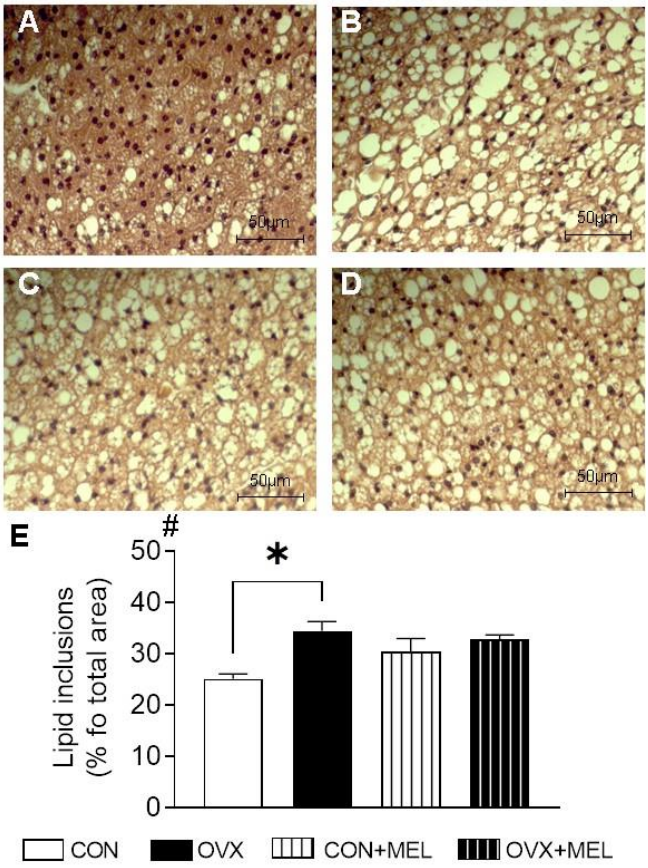

Fig. 5. Effects of OVX and MEL on photomicrography of brown adipose tissue (BAT).

*BAT was stained with H&E. A. BAT of CON rats. B. BAT of OVX rats. C. BAT of CON+MEL rats. D. BAT of OVX+MEL rats. E. The area occupied by vesicles in the four groups, expressed as a percentage of the total area of the tissues. MEL: melatonin, CON: sham-operated rats, OVX: ovariectomized rats, CON+MEL: MEL-treated control rats, OVX+MEL: MEL-treated OVX rats. All data are expressed as the mean ± SE of 3–4 individual experiments. The significant differences were evaluated using a two-way analysis of variance (ANOVA) with Tukey's post-hoc test: * $p \leq 0.05$; #: Significant main effect of animal condition (CON x OVX).*

3.4. Effects of OVX and MEL on parameters of oxidative stress in retroperitoneal, inguinal, and brown ATs.

The redox status of the ATs was evaluated by measuring the levels of TBARS in the total homogenate and the content of GSH and thiols in the cytosolic soluble fraction. In rVAT (Figure 6 A, D, G) and BAT (Figure 6 C, F, I), none of these three parameters were significantly different among the four groups, except for a decrease in TBARS content in CON+MEL rats (-29%) compared to CON rats (Figure 6 A). In iSAT, the content of TBARS and thiols was not altered in OVX rats (Figure 6 B, H), but a decrease of 70% was found in the GSH content compared to CON rats (Figure 6 E). MEL administration in OVX rats leads to the restoration

of GSH content (Figure 6 E) and increased the thiol content in CON+MEL rats (+71%; Figure 6 H) compared to their respective untreated controls.

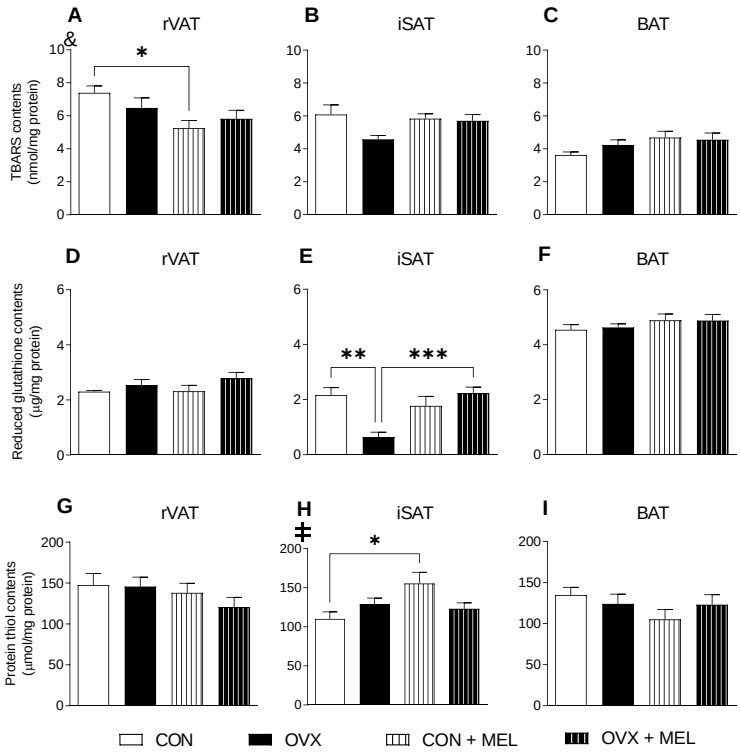

Fig. 6. Effects of OVX and MEL on the parameters of oxidative stress in adipose tissues (ATs).

*A, B, C. The TBARS content in total homogenate. D, E, F. The reduced glutathione (GSH) content in the cytosolic fraction. G, H, I. The protein thiol content in the cytosolic fraction. rVAT: retroperitoneal visceral adipose tissues, iSAT: inguinal subcutaneous adipose tissues; BAT: brown adipose tissues, MEL: melatonin, CON: sham-operated rats, OVX: ovariectomized rats, CON+MEL: MEL-treated control rats, OVX+MEL: MEL-treated OVX rats. The values are expressed as the mean ± SE of 4–12 individual experiments. The significant differences were evaluated using a two-way analysis of variance (ANOVA) with Tukey's post-hoc test: * $p \leq 0.05$; ** $p \leq 0.01$; *** $p \leq 0.001$. &: Significant main effect of treatment (Saline x MEL); ‡: Significant interaction between animal condition (CON x OVX) and treatment (Saline x MEL). Data from panel E were analyzed by one-way non-parametric ANOVA with Kruskal-Wallis test.*

The activities of antioxidant enzymes in rVAT, iSAT, and BAT are shown in Figure 7. OVX caused the significant changes only in the iSAT: the GR and G6PD activities reduced 44% (Figure 7 K) and 41% (Figure 7 N), respectively, compared to CON rats. These results agreed with the reduced content of GSH found in this tissue (Figure 6 E). The MEL treatment restored the activities of these two enzymes to values (Figure 7 K, N) similar to those of CON rats.

In rVAT, although the activities of GSH-Px (Figure 7 G) and GR (Figure 7 J) were not significantly altered in OVX rats compared to CON rats, the administration of MEL to these rats (OVX+MEL) increased the activity of both enzymes by approximately 36% compared to OVX rats. MEL administration in the CON rats did not exert significant changes in any of the assayed enzymes in the three ATs. In BAT, these enzymes were not affected by ovariectomy or MEL treatment (Figure 7 C, F, I, L, O).

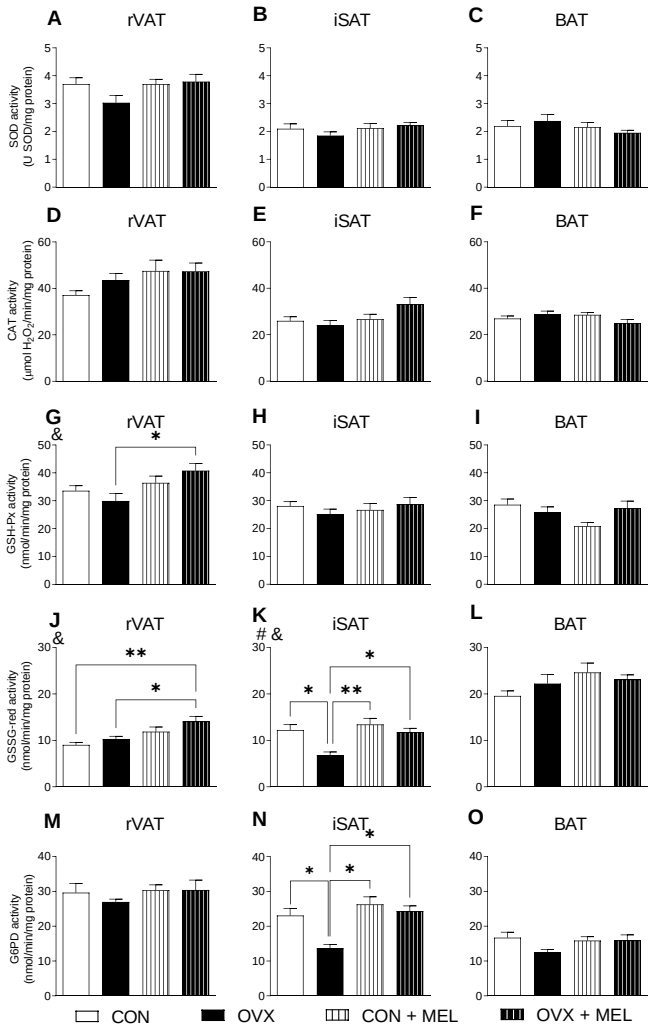

Fig. 7. Effects of OVX and MEL on the activities of antioxidant enzymes in adipose tissues (ATs).

*A, B, C. The superoxide dismutase (SOD) activity. D, E, F. The catalase (CAT) activity. G, H, I. The glutathione peroxidase (GPx) activity. J, K, L. The glutathione reductase (GR) activity. M, N, O. The glucose-6-phosphate dehydrogenase (G6PD) activity. rVAT: retroperitoneal visceral adipose tissues, iSAT: inguinal subcutaneous adipose tissues, BAT: brown adipose tissues, MEL: melatonin, CON: sham-operated rats, OVX: ovariectomized rats, CON+MEL: MEL-treated control rats, OVX+MEL: MEL-treated OVX rats. The values are the mean ± SE of 3–7 individual experiments. The significant differences were evaluated using a two-way analysis of variance (ANOVA) with Tukey's post-hoc test. * $p \leq 0.05$; ** $p \leq 0.01$; *** $p \leq 0.001$. #: Significant main effect of animal condition (SHAM x OVX); &: Significant main effect of treatment (Saline x MEL). Data from panel N were analyzed by one-way non-parametric ANOVA with Kruskal-Wallis test.*

4. DISCUSSION

In the present study, we have found that after 16 weeks of ovariectomy, the female rats had reduced serum levels of estradiol and showed sign of uterine atrophy, and some components of the MetS (60), including the BW gaining and increased adiposity. The increased fat accumulation in OVX rats was not correlated with food consumption, confirming the results of our previous studies (28, 61, 62). Dyslipidemia, hyperglycemia and insulinemia in OVX

rodents have been reported in some studies (61, 63), but not in others (28, 62, 64) which were consistent with the results observed in our experimental conditions. Indeed, nearly 50% to 80% of women in the menopausal and postmenopausal periods remain healthy despite the loss of estrogen protection, with the other proportion developing one or more components of MetS (35, 36, 65, 66).

The increase in corporal lipid accounted for most of the BW gaining in OVX rats compared to the CON rats. Among the assayed ATs, the increase in the weight of iSAT determined the higher adiposity indexes. The morphology of visceral (VAT) and subcutaneous (SAT) fat revealed significant alterations in the plasticity of these ATs due to estrogen deficiency. In the rVAT, a significant increase in adipocyte area (hypertrophy) was observed without a change in total fat mass. A distinct phenomenon occurred in iSAT, in which adipocytes exhibited a similar size to those of the control rats, but, were associated with a substantial increase in their mass, a sign of iSAT hyperplasia.

The predominance of hypertrophic cells in rVAT may be a consequence of the change in receptor-mediated action of estrogen, as suggested by hypertrophy of perigonadal fat pads in ER alpha (ERα) knockout mice (67). The receptor-mediated actions of estrogen in ATs occur through the classic ERα and beta (ERβ) and non-classic G protein-coupled estrogen receptors (GPER) E2 receptors, with ERα having a major influence (36, 67). A protective role of ERα against metabolic disturbances has been demonstrated (67), but the role of ERβ in adipose tissues is less understood. Ahmed *et al*. (36) demonstrated depot-specific differences in the expression of ERα and ERβ in pre- and postmenopausal women. Whereas in premenopausal women ERα expression is higher in VAT compared to SAT, ERβ is lower in VAT than in SAT in both pre- and postmenopausal women. The authors also found an increased ERβ expression only in SAT of postmenopausal women. It is unknown whether differences in estrogen receptors (ERs) affect the morphology and functions of adipocytes in different fat depots in rats. However, a considerable difference in morphological change due to ovariectomy was found in iSAT compared to VAT, as the increase in iSAT mass was associated with decreased adipocyte area.

Studies have demonstrated that once the maximal lipid accumulation is reached (hypertrophy) in adipocytes, the hyperplastic growth is initiated in both VAT and SAT. The expansion of ATs by enhanced adipogenesis distributes excess fat between newly differentiated adipocytes and protects against ectopic fat deposition (68, 69). This phenomenon appears to occur in iSAT, as there was a substantial increase in its mass without a change in the mean adipocyte size.

The intracellular redox state regulated by the levels of GSSG/GSH, thioredoxin, and cysteine (70), as well as ROS and the NADPH oxidase 4 (Nox4)-generated H_2O_2 (37), exerts great influence on AT functions, such as adipogenesis; however, an imbalance in the redox state leads to an oxidative stress and adipocyte dysfunctions (40, 71, 72). The adequate balance of the redox state depends on a battery of antioxidant enzymes. The cytosolic and mitochondrial SODs catalyze the the dismutation of superoxide anion ($O_2^{\cdot -}$) into hydrogen peroxide (H_2O_2), while CAT and GPx remove the H_2O_2 (71, 72). GPx requires reduced GSH for activity (43), and GR reduces the oxidized GSSG using the reductive force of NADPH to restore GSH levels (73). NADPH is generated by the pentose phosphate pathway in the first step catalyzed by G6PD (74).

In rVAT and BAT from OVX rats, none of these enzymes, as well as the parameters indicative of cellular redox state, including the content of MDA, thiol proteins, and GSH were significantly different from those of CON rats. In rVAT, despite exhibiting an increase in the size of adipocytes, the maximal capacity of lipid accumulation was likely not exceeded, preventing a disturbance in the redox state. A transfer of excess lipids from VAT to subcutaneous ATs and the liver may have contributed to preventing VAT adipocyte

dysfunction, as suggested by the iSAT hyperplasia and hepatic steatosis (28). However, in iSAT, ovariectomy caused a decrease in the GSH content. An inhibition in the reduction of GSSG to GSH in OVX rats was suggested by the reduced activity of GR and G6PD. These alterations can also be consequences of estrogen deficiency. In addition to acting as a ROS scavenger (41), estrogens exert receptor-mediated protection against oxidative stress by increasing the levels of GSH and the expression of antioxidant enzymes, including SOD, GR, G6PD, and GPx (46). Regardless of this change in GSH, no significant oxidative damage was observed since as the MDA and thiol proteins were not altered and iSAT growth was not compromised.

Despite the ovary removal, the plasmatic estradiol levels of OVX rats remained 25% of the values observed in CON rats. This occurs due to the extragonadal production of estrogen from androgen precursors in tissues such as the brain, AT, placenta, blood vessels, skin, and bone (75). The rate-limiting step in this reaction is catalyzed by the cytochrome P450 enzyme aromatase, which converts 19-carbon steroids (e.g., androgens androstenedione and testosterone) to 18-carbon steroids (e.g., estrogens estrone and estradiol) (75). In postmenopausal women, VATs become the primary source of estrogens (76, 77) to partly compensate for the reduced ovarian estrogen secretion (77). Despite being hypertrophic, adipocytes of rVAT in OVX rats exhibited no signs of redox state disruption, most likely due to the protective effect of local estrogen secretion.

Similar to estrogen, MEL is also a potent antioxidant due to directly neutralizing ROS and indirectly activating antioxidant enzymes (15, 44, 45). MEL freely crosses the morpho-physiological barriers, reaching many organs, including the brain (78). In peripheral tissues, MEL interacts with receptors, including the MT1, MT2, and MT3 (79, 80), the retinoid Z receptors (RZRs) (81), and intracellular calmodulin (82).

In females under normoestrogenic conditions (CON rats), MEL decreased body weight and adiposity. The effects of MEL in reducing BW, adiposity and other manifestations of MetS (16) have been extensively studied in obese patients and experimental model of rodents with obesity and diabetes (17-19). The actions of melatonin have been shown to involve multiple levels, including stimulation of adipocyte lipolysis through activation of the sympathetic nervous system (83); change in preadipocyte differentiation and adipogenesis (84-86); increase in insulin sensitivity (87), thermogenic capacity and energy expenditure through BAT growth (88); browning WAT to beige adipogenesis (18); neutralizing inflammatory infiltration and adipokine alteration (89-92); reduction of oxidative damage (93) and modulation of the intestinal microbiota (94).

A reduction in BW by MEL in a normoestrogenic condition agreed with previous reports (95-97), but the molecular mechanism by which MEL reduces BW and food intake is not entirely understood. In several studies, a change in food intake has not been evidenced (88, 97, 98). The involvement of leptin is unclear since a decrease (95, 97), increase (99), or lack of changes (100) in plasmatic leptin levels have been reported in MEL-treated rats. An extra energy demand due to increased nocturnal activity has been suggested as a factor leading to a decrease in body adiposity (97).

In our study, MEL only decreased the mVAT mass in normoestrogenic conditions. The mass of rVAT, iSAT, and BAT was not altered, nor was the morphology of rVAT adipocytes. However, MEL induced morphogenic changes in iSAT, resulting in a significant increase in the proportion of small cells. As the total mass remained unchanged, an increase in the formation of new adipocytes in iWAT may represent a mechanism by which MEL promotes a more even distribution of lipids among the ATs. This finding was in agreement with the *in vitro* study on 3T3-L1 preadipocytes, which demonstrated that MEL promotes adipogenesis and accumulation of triglyceride during preadipocyte differentiation (86).

Increased fatty acid oxidation may have contributed to the decrease in the adiposity and BW of CON+MEL rats. By acting on MT1 receptors in the suprachiasmatic nucleus neurons, MEL activates sympathetic drive in various peripheral tissues, including WAT, BAT, liver, adrenal medulla and skeletal muscle (19, 101), which can elicit acute catabolic responses such as lipolysis and fatty acid oxidation (101, 102). Liu *et al*. (101) showed that MEL decreases intramuscular fat in the *vastus lateralis* muscle of the mouse hind limb by positively regulating lipolysis and mitochondrial activities. Recently, Salagre *et al*. (19) demonstrated that melatonin improves obesity in fatty Zücker diabetic rats by inducing the thermogenic capacity of skeletal muscle, an action mediated by uncoupling of sarcoendoplasmic reticulum Ca^{2+}-ATPase (SERCA)-sarcolipin (SLN) and mitochondrial biogenesis.

An increase in energy expenditure due to increased fatty acid oxidation in BAT (18, 103) or browning of iSAT (18) has also been suggested as a mechanism of MEL in reducing adiposity (101). We have not found differences in the area occupied by lipids in the BAT of CON+MEL rats, but an increase in the rate of lipid oxidation cannot be excluded.

We also found in CON rats treated with MEL (CON+MEL) reduced plasma estradiol levels compared to CON rats. The uterine mass was also reduced, as the uterus is a classic estrogen-responsive target tissue. These findings are in line with studies showing that MEL negatively regulates ER expression, preventing ER-mediated gene activation and inhibiting the gonadotropic axis (104, 105). MEL also inhibits the expression and activity of enzymes involved in estrogen biosynthesis in peripheral tissues, particularly aromatase (106).

Under estrogen deficiency, the putative mechanisms by which MEL decreased the body weight in female rats were no longer effective since the BW and adiposity of OVX rats were not suppressed by MEL. This result was similar to our previous study, in which MEL was administered after 13 weeks of ovariectomy (28). The reason for such difference is likely related to estrogen levels in the rats. The regulation of body weight and feeding behavior involves a complex interaction of hormones, their receptors in the SNC and peripheral tissues (24). Both estrogen and melatonin regulate energy homeostasis and obesity at the central and peripheral levels (8, 24), and an interaction of MEL with sex steroid hormones and *vice versa* has become clear (107). MEL, for example, regulates the secretion of FSH and LH through the hypothalamic-pituitary-gonadal axis, and affects steroidogenesis, ovulation and oocyte quality (108). It seems plausible to suggest that some actions of exogenous MEL in regulating body adiposity involve an interaction with estrogens, particularly in females under normoestrogenic conditions.

Despite not decreasing whole-body adiposity in OVX rats, MEL changes the morphology of the ATs in both rVAT and iSAT toward a healthier condition. MEL suppressed the adipocyte hypertrophy observed in the rWAT of OVX rats. This effect could be a consequence of increased lipolysis, as MEL up-regulates the expression of lipolytic genes via the MT2 receptor, including hormone-sensitive lipase, triglyceride, and perilipin 1 (109). In reducing the lipid load and massive expansion of adipocytes in rVAT, MEL can prevent and minimize the risk of of hypoxia, inflammation, and ectopic lipid deposition, a phenomenon that may have contributed to the suppression of hepatic steatosis in OVX rats, as previously demonstrated (28).

MEL also did not suppress the increase in iSAT weight of OVX mice, but the morphology of adipocytes changed toward a prevalence of small adipocytes, reproducing the effect observed in iSAT of CON rats. This result reinforces the notion that MEL has a direct effect on iSAT, stimulating adipogenesis (85).

The restoration of the redox state of iSAT corroborated this beneficial effect of MEL in the ATs of OVX rats. The decrease in the GSH levels and GR and G6PD activities in iSAT was suppressed by MEL, and MEL exerted additional effects on the antioxidant defense systems, as indicated by the activity of GPx and GR in rVAT, with all these enzymes reaching levels

higher than the values found in both CON and OVX rats. These effects were in agreement with the activation of glutathione synthesis and antioxidant enzymatic activity by MEL (15, 44). All these results support the antioxidant role of MEL in replacing the estrogens.

In conclusion, this study revealed that, despite not preventing the increase in body adiposity, MEL administration was able to suppress most of the alterations in adipose morphology and redox state caused by estrogen deficiency in rats, leading to a better distribution of lipids in the ATs. In clear contrast to the effect observed in OVX rats, under normoestrogenic conditions, MEL reduced the BW, adiposity, plasma estradiol levels, and uterine weight. These findings suggest that in estrogen deficiency conditions, MEL administration can minimize the risks of developing more severe metabolic abnormalities, whereas in normoestrogenic conditions, MEL can potentially affect the estrogen-regulated functions, including the control of body energy homeostasis and reproduction.

ACKNOWLEDGEMENTS

This work was supported by the Coordenação de Aperfeiçoamento de Pessoal do Ensino Superior (CAPES), grants CAPES/NUFFIC 14/10; and the Conselho Nacional de Desenvolvimento Científico e Tecnológico (CNPq), grants 303927/2013-5. Danielle Aparecida Munhos Hermoso has received a doctoral fellowship from the Conselho Nacional de Desenvolvimento Científico e Tecnológico (CNPq), 142257/2015-0.

AUTHORSHIP

Conceptualization: Emy Luiza Ishii Iwamoto, Rodrigo Polimeni Constantin and Eduardo Hideo Gilglioni; Methodology: Danielle Aparecida Munhos Hermoso, Tatiana Carlesso dos Santos, Maria Raquel Marçal Natali, Lenilson da Fonseca Roza and Aparecida Pinto Munhos Hermoso; Formal analysis and investigation: Danielle Aparecida Munhos Hermoso, Emy Luiza Ishii Iwamoto; Eduardo Makiwama Klosowski and Franciele Neves Moreno; Writing - original draft preparation: Emy Luiza Ishii Iwamoto, Danielle Aparecida Munhos Hermoso, Eduardo Hideo Gilglione, and other authors commented on previous versions of the manuscript; Writing – review and editing: Emy Luiza Ishii Iwamoto; Funding acquisition: Emy Luiza Ishii Iwamoto and Danielle Aparecida Munhos Hermoso; Supervision: Emy Luiza Ishii Iwamoto. All authors read and approved the manuscript.

CONFLICT OF INTEREST STATEMENT

The authors declare that there are no conflicts of interest.

REFERENCES

1. Borjigin J, Zhang LS, Calinescu AA (2012) Circadian regulation of pineal gland rhythmicity. *Mol. Cell Endocrinol.* **349** (1): 13-19. https://www.ncbi.nlm.nih.gov/pubmed/21782887.
2. Lopez-Gonzalez MA, Calvo JR, Segura JJ, Guerrero JM (1993) Characterization of melatonin binding sites in human peripheral blood neutrophils. *Biotechnol. Ther.* **4** (3-4): 253-262. https://www.ncbi.nlm.nih.gov/pubmed/8292973.
3. Faillace MP, Cutrera R, Sarmiento MI, Rosenstein RE (1995) Evidence for local synthesis of melatonin in golden hamster retina. *Neuroreport* **6** (15): 2093-2095. https://www.ncbi.nlm.nih.gov/pubmed/8580448.

4. Tan DX, Manchester LC, Reiter RJ, Qi WB, Zhang M, Weintraub ST, Cabrera J, Sainz RM, Mayo JC, (1999) Identification of highly elevated levels of melatonin in bone marrow: its origin and significance. *Biochim. Biophys. Acta* **1472** (1-2): 206-214. https://www.ncbi.nlm.nih.gov/pubmed/10572942.
5. Lardone PJ, Carrillo-Vico A, Molinero P, Rubio A, Guerrero JM (2009) A novel interplay between membrane and nuclear melatonin receptors in human lymphocytes: significance in IL-2 production. *Cell Mol. Life Sci.* **66** (3): 516-525. https://www.ncbi.nlm.nih.gov/pubmed/19099187.
6. Conti A, Conconi S, Hertens E, Skwarlo-Sonta K, Markowska M, Maestroni JM (2000) Evidence for melatonin synthesis in mouse and human bone marrow cells. *J. Pineal Res.* **28** (4): 193-202. https://www.ncbi.nlm.nih.gov/pubmed/10831154.
7. Huether G, Poeggeler B, Reimer A, George A (1992) Effect of tryptophan administration on circulating melatonin levels in chicks and rats: evidence for stimulation of melatonin synthesis and release in the gastrointestinal tract. *Life Sci.* **51** (12): 945-953. https://www.ncbi.nlm.nih.gov/pubmed/1518369.
8. Roy D, Belsham DD (2002) Melatonin receptor activation regulates GnRH gene expression and secretion in GT1-7 GnRH neurons. Signal transduction mechanisms. *J. Biol. Chem.* **277** (1): 251-258. https://www.ncbi.nlm.nih.gov/pubmed/11684691.
9. Reiter RJ, Tamura H, Tan DX, Xu XY (2014) Melatonin and the circadian system: contributions to successful female reproduction. *Fertil. Steril.* **102** (2): 321-328. https://www.ncbi.nlm.nih.gov/pubmed/24996495.
10. Lobo RA (2008) Metabolic syndrome after menopause and the role of hormones. *Maturitas* **60** (1): 10-18. https://www.ncbi.nlm.nih.gov/pubmed/18407440.
11. Cagnacci A,, Arangino S, Angiolucci M, Melis GB, Tarquini R, Renzi A, Volpe A (2000) Different circulatory response to melatonin in postmenopausal women without and with hormone replacement therapy *J. Pineal Res*. **29** (3): 152-158. https://www.ncbi.nlm.nih.gov/pubmed/11034112.
12. Greendale GA, Witt-Enderby P, Karlamangla AS, Munmun F, Crawford S, Huang MH, Santoro N (2020) Melatonin patterns and levels during the human menstrual cycle and after menopause. *J. Endocr. Soc.* **4** (11): bvaa115. https://www.ncbi.nlm.nih.gov/pubmed/33094207.
13. Lima FB, Machado UF, Bartol I, Seraphim PM, Sumida DH, Moraes SM, Hell NS, Okamoto MM, Saad MJ, Carvalho CR, Cipolla-Neto J (1998) Pinealectomy causes glucose intolerance and decreases adipose cell responsiveness to insulin in rats. *Am. J. Physiol.* **275** (6) :E934-941. https://www.ncbi.nlm.nih.gov/pubmed/9843734.
14. Bellipanni G, Bianchi P, Pierpaoli W, Bulian D, Ilyia E (2001) Effects of melatonin in perimenopausal and menopausal women: a randomized and placebo controlled study. *Exp. Gerontol.* **36** (2): 297-310. https://www.ncbi.nlm.nih.gov/pubmed/11226744.
15. Chojnacki C, Kaczka A, Gasiorowska A, Fichna J, Chojnacki J, Brzozowski T (2018) The effect of long-term melatonin supplementation on psychosomatic disorders in postmenopausal women. *J. Physiol. Pharmacol.* **69** (2): 297-304. https://www.ncbi.nlm.nih.gov/pubmed/30045006.
16. Delpino FM, Figueiredo LM (2021) Melatonin supplementation and anthropometric indicators of obesity: A systematic review and meta-analysis. *Nutrition* **91-92**:111399. https://www.ncbi.nlm.nih.gov/pubmed/34626955.
17. Genario R, Cipolla-Neto J, Bueno AA, Santos HO (2021) Melatonin supplementation in the management of obesity and obesity-associated disorders: A review of physiological mechanisms and clinical applications. *Pharmacol. Res.* **163**: 105254. https://www.ncbi.nlm.nih.gov/pubmed/33080320.

18. Jimenez-Aranda A, Fernandez-Vazquez G, Campos D, Tassi M, Velasco-Perez L, Tan DX, Reiter RJ, Agil A (2013) Melatonin induces browning of inguinal white adipose tissue in Zucker diabetic fatty rats. *J. Pineal Res.* **55** (4): 416-423. https://www.ncbi.nlm.nih.gov/pubmed/24007241.
19. Salagre D, Navarro-Alarcón M, Villalón-Mir M, Alcázar-Navarrete B, Gómez-Moreno G, Tamimi F, Agil A (2024) Chronic melatonin treatment improves obesity by inducing uncoupling of skeletal muscle SERCA-SLN mediated by CaMKII/AMPK/PGC1α pathway and mitochondrial biogenesis in female and male Zücker diabetic fatty rats. *Biomed. Pharmacother*. **172**: 116314. https://pubmed.ncbi.nlm.nih.gov/38387135.
20. Asarian L, Geary N (2002) Cyclic estradiol treatment normalizes body weight and restores physiological patterns of spontaneous feeding and sexual receptivity in ovariectomized rats. *Horm. Behav.* **42** (4): 461-471. https://www.ncbi.nlm.nih.gov/pubmed/12488112.
21. Baxi D, Singh PK, Vachhrajani K, Ramachandran AV (2012) Melatonin supplementation therapy as a potent alternative to ERT in ovariectomized rats. *Climacteric* **15** (4): 382-392. https://www.ncbi.nlm.nih.gov/pubmed/22185471.
22. Finan B, Yang B, Ottaway N, Stemmer K, MüllerTD, Yi XC, Habegger K, Schriever S C, García-CA, Kabra DG (2012) Targeted estrogen delivery reverses the metabolic syndrome. *Nat. Med.* **18** (12): 1847-1856. https://www.ncbi.nlm.nih.gov/pubmed/23142820.
23. Mahboobifard F, Pourgholami MH, Jorjani M, Dargahi L, Amiri M, Sadeghi S, Tehrani FR (2022) Estrogen as a key regulator of energy homeostasis and metabolic health. *Biomed. Pharmacoter.* **156**: 113808. https://www.ncbi.nlm.nih.gov/pubmed/36252357.
24. Xu Y, López M (2018) Central regulation of energy metabolism by estrogens. *Mol. Metab.* **15**: 104-115. https://www.ncbi.nlm.nih.gov/pubmed/29886181.
25. Amstrup AK, Sikjaer T, Pedersen, SB, Heickendorff L, Mosekilde L, Rejnmark L (2016) Reduced fat mass and increased lean mass in response to 1 year of melatonin treatment in postmenopausal women: A randomized placebo-controlled trial. *Clin. Endocrinol.* **84** (3): 342-347. https://www.ncbi.nlm.nih.gov/pubmed/26352863.
26. Hsu LW, Chien YW (2023) Effects of melatonin supplementation on lipid metabolism and body fat accumulation in ovariectomized rats. *Nutrients* **15** (12): 2800. https://www.ncbi.nlm.nih.gov/pubmed/37375706.
27. Sanchez-Mateos S, Alonso-Gonzalez C, Gonzalez A, Martinez-Campa CM, Mediavilla MD, Cos S, Sanchez-Barcelo EJ, *et al.* (2007) Melatonin and estradiol effects on food intake, body weight, and leptin in ovariectomized rats. *Maturitas* **58** (1): 91-101. https://www.ncbi.nlm.nih.gov/pubmed/17706901.
28. Hermoso, DAM, Shimada LBC, Gilglioni EH, Constantin J, Mito MS, Hermoso APM, Salgueiro-Pagadigorria CL, Iwamoto ELI. (2016) Melatonin protects female rats against steatosis and liver oxidative stress induced by oestrogen deficiency. *Life Sci.* **157**: 178-186. https://www.ncbi.nlm.nih.gov/pubmed/27262788.
29. Hoffstedt J, Arner E, Wahrenberg H, Andersson DP, Qvisth V, Lofgren P, Ryden M, Thorne A, Wiren M, Palmer M, Thorell A, Toft E, Arner P (2010) Regional impact of adipose tissue morphology on the metabolic profile in morbid obesity. *Diabetologia* **53** (12): 2496-2503. https://www.ncbi.nlm.nih.gov/pubmed/20830466.
30. Zhang M, Hu T, Zhang S, Zhou L (2015) Associations of different adipose tissue depots with insulin resistance: A systematic review and meta-analysis of observational studies. *Sci. Rep.* **5**:18495. https://www.ncbi.nlm.nih.gov/pubmed/26686961.
31. Fang L, Guo F, Zhou L, Stahl R, Grams J (2015) The cell size and distribution of adipocytes from subcutaneous and visceral fat is associated with type 2 diabetes mellitus in humans. *Adipocyte* **4** (4): 273-279. https://www.ncbi.nlm.nih.gov/pubmed/26451283.
32. Le Gouic S, Atgié C, Viguerie-Bascands N, Hanoun N, Larrouy D, Ambid L, Raimbault S, Ricquier D, Delagrange P, Guardiola-Lemaitre B, Pénicaud L, Casteilla L (1997)

Characterization of a melatonin binding site in Siberian hamster brown adipose tissue. *Eur. J. Pharmacol.* **339** (2-3): 271-278. https://www.ncbi.nlm.nih.gov/pubmed/9473145.
33. Lovejoy JC, Sainsbury A, Stock Conference Working G (2009) Sex differences in obesity and the regulation of energy homeostasis. *Obes. Rev.* **10** (2): 154-167. https://www.ncbi.nlm.nih.gov/pubmed/19021872.
34. Macotela Y, Boucher J, Tran TT, Kahn CR (2009) Sex and depot differences in adipocyte insulin sensitivity and glucose metabolism. *Diabetes* **58** (4): 803-812. https://www.ncbi.nlm.nih.gov/pubmed/19136652.
35. Abildgaard J, Danielsen ER, Dorph E, Thomsen C, Juul A, Ewertsen C, Pedersen BK, Pedersen AT, Ploug T, Lindegaard B (2021) Changes in abdominal subcutaneous adipose tissue phenotype following menopause is associated with increased visceral fat mass. *Sci. Rep.* **11** (1): 14750. ://www.ncbi.nlm.nih.gov/pubmed/34285301.
36. Ahmed, Kamble PG, Hetty S, Fanni G, Milica M, Sarsenbayeva A, Kristófi R, Svensson MK, Pereira MJ, Eriksson JW (2022) Role of estrogen and its receptors in adipose tissue glucose metabolism in pre- and postmenopausal women. *J. Clin. Endocrinol. Met.* **107** (5): e1879-e1889. https://www.ncbi.nlm.nih.gov/pubmed/35084504.
37. Castro JP, Grune T, Speckmann B (2016) The two faces of reactive oxygen species (ROS) in adipocyte function and dysfunction. *Biol. Chem.* **397** (8): 709-724. https://www.ncbi.nlm.nih.gov/pubmed/27031218.
38. Murdolo G, Piroddi M, Luchetti F, Tortoioli C, Canonico B, Zerbinati C, Galli F, Iuliano L (2013) Oxidative stress and lipid peroxidation by-products at the crossroad between adipose organ dysregulation and obesity-linked insulin resistance. *Biochimie* **95** (3): 585-594. https://www.ncbi.nlm.nih.gov/pubmed/23274128.
39. Becker BN, Himmelfarb J, Henrich WL, Hakim RM (1997) Reassessing the cardiac risk profile in chronic hemodialysis patients: a hypothesis on the role of oxidant stress and other non-traditional cardiac risk factors. *J. Am. Soc. Nephrol.* **8** (3): 475-486. https://www.ncbi.nlm.nih.gov/pubmed/9071717.
40. Doshi SB, Agarwal A (2013) The role of oxidative stress in menopause. *J. Midlife Health* **4** (3): 140-146. https://www.ncbi.nlm.nih.gov/pubmed/24672185.
41. Behl C, Skutella T, Lezoualc'h F, Post A, Widmann M, Newton CJ, Holsboer F (1997) Neuroprotection against oxidative stress by estrogens: structure-activity relationship. *Mol. Pharmacol.* **51** (4): 535-541. https://www.ncbi.nlm.nih.gov/pubmed/9106616.
42. Borrás C, Gambini J, Gomez-Cabrera MC, Sastre J, Pallardo FV, Mann GE, Vina J (2005) 17beta-oestradiol up-regulates longevity-related, antioxidant enzyme expression via the ERK1 and ERK2[MAPK]/NFkappaB cascade. *Aging cell* **4** (3): 113-118. https://www.ncbi.nlm.nih.gov/pubmed/15924567.
43. Garcia-Ruiz C, Fernandez-Checa JC (2018) Mitochondrial oxidative stress and antioxidants balance in fatty liver disease. *Hepatol. Commun.* **2** (12): 1425-1439. https://www.ncbi.nlm.nih.gov/pubmed/30556032.
44. Suzen S, Atayik MC, Sirinzade H, Entezari B, Gurer-Orhan H, Çakatay U (2022) Melatonin and redox homeostasis. *Melatonin Res*. **5** (3): 304-324.
45. Reiter RJ, Tan DX, Terron MP, Flores LJ, Czarnocki Z (2007) Melatonin and its metabolites: new findings regarding their production and their radical scavenging actions. *Acta Biochim. Pol.* **54** (1): 1-9. https://www.ncbi.nlm.nih.gov/pubmed/17351668.
46. García JJ, Lopez-Pingarron L, Almeida-Souza P, Tres A, Escudero P, Garcia-Gil FA, Tan DX, Reiter RJ, Ramirez JM, Bernal-Perez M (2014) Protective effects of melatonin in reducing oxidative stress and in preserving the fluidity of biological membranes: A review. *J. Pineal Res.* **56** (3): 225-237. https://www.ncbi.nlm.nih.gov/pubmed/24571249.

47. Folch J, Lees M, Sloane Stanley GH (1957) A simple method for the isolation and purification of total lipides from animal tissues. *J. Biol. Chem.* **226** (1): 497-509. https://www.ncbi.nlm.nih.gov/pubmed/13428781.
48. Latimer GW (2016) *Official methods of analysis of AOAC International* 20 Ed.
49. Marcondes FK, Biachi FJ, Tanno AP (2002) Determination of the estrous cycle phases of rats some helpful considerations. *Braz. J. Biol.* **62**: 609-614.
50. Smith MS, Freeman ME, Neill JD (1975) The control of progesterone secretion during the estrous cycle and early pseudopregnancy in the rat: prolactin, gonadotropin and steroid levels associated with rescue of the corpus luteum of pseudopregnancy. *Endocrinology* **96** (1): 219-226. https://www.ncbi.nlm.nih.gov/pubmed/1167352.
51. Friedewald W, Levy Ra, Fredrickson D (1972) Estimation of the concentration of low-density lipoprotein cholesterol in plasma, without use of the preparative ultracentrifuge. *Clin. Chem.* **18**: 499-502.
52. Ohkawa H, Ohishi N, Yagi K (1979) Assay for lipid peroxides in animal tissues by thiobarbituric acid reaction. *Anal. Biochem.* **95** (2): 351-358. https://www.ncbi.nlm.nih.gov/pubmed/36810.
53. Sedlak J, Lindsay RH (1968) Estimation of total, protein-bound, and nonprotein sulfhydryl groups in tissue with Ellman's reagent. *Anal. Biochem.* **25**: 192-205. https://doi.org/10.1016/0003-2697(68)90092-4.
54. Hissin PJ, Hilf R (1976) A fluorometric method for determination of oxidized and reduced glutathione in tissues. *Anal. Biochem.* **74** (1): 214-226. Https://www.ncbi.nlm.nih.gov/pubmed/962076.
55. Marklund S, Marklund G (1974) Involvement of the superoxide anion radical in the autoxidation of pyrogallol and a convenient assay for superoxide dismutase. *Eur. J. Biochem.* **47** (3): 469-474. https://www.ncbi.nlm.nih.gov/pubmed/4215654.
56. Paglia DE, Valentine WN (1967) Studies on the quantitative and qualitative characterization of erythrocyte glutathione peroxidase. *J. Lab. Clin. Med*. **70** (1): 158-169. https://www.ncbi.nlm.nih.gov/pubmed/6066618.
57. Mize CE, Langdon RG (1962) Hepatic glutathione reductase. I. Purification and general kinetic properties. *J. Biol. Chem.* **237**: 1589-1595. https://www.ncbi.nlm.nih.gov/pubmed/14474846.
58. Aebi H, Wyss SR, Scherz B, Skvaril F (1974) Heterogeneity of erythrocyte catalase II. Isolation and characterization of normal and variant erythrocyte catalase and their subunits. *Eur. J. Biochem.* **48** (1): 137-145. https://www.ncbi.nlm.nih.gov/pubmed/4141308.
59. Tian WN, Pignatare JN, Stanton RC (1994) Signal transduction proteins that associate with the platelet-derived growth factor (PDGF) receptor mediate the PDGF-induced release of glucose-6-phosphate dehydrogenase from permeabilized cells. *J. Biol. Chem.* **269** (20): 14798-14805.
60. Kaur J (2014) A comprehensive review on metabolic syndrome. *Cardiol. Res. Pract.* **2014**: 943162. https://www.ncbi.nlm.nih.gov/pubmed/24711954.
61. Campos LB, Gilglioni EH, Garcia RF, Brito MN, Natali MR, Ishii-Iwamoto EL, Salgueiro-Pagadigorria CL (2012) Cimicifuga racemosa impairs fatty acid beta-oxidation and induces oxidative stress in livers of ovariectomized rats with renovascular hypertension. *Free Radic. Biol. Med.* **53** (4):.680-689. https://www.ncbi.nlm.nih.gov/pubmed/22684021.
62. Gilglioni EH, Campos LB, Oliveira MC, Garcia RF, Ambiel CR, Buzzo AJ, Ishii-Iwamoto E, Salgueiro-Pagadigorria CL (2013) Beneficial effects of tibolone on blood pressure and liver redox status in ovariectomized rats with renovascular hypertension. *J. Geronto..A Biol. Sc.i Med. Sci*. **68** (5): 510-520. https://www.ncbi.nlm.nih.gov/pubmed/23089337.

63. Abbas AM, Elsamanoudy AZ (2011) Effects of 17beta-estradiol and antioxidant administration on oxidative stress and insulin resistance in ovariectomized rats. *Can. J. Physiol. Pharmacol.* **89** (7): 497-504. https://www.ncbi.nlm.nih.gov/pubmed/21812527.
64. Camporez JP, Jornayvaz FR, Lee HY, Kanda S, Guigni BA, Kahn M, Samuel V, Carvalho CRO, Petersen KF, Jurczak MJ, Shulman GI (2013) Cellular mechanism by which estradiol protects female ovariectomized mice from high-fat diet-induced hepatic and muscle insulin resistance. *Endocrinology* **154** (3): 1021-1028. https://www.ncbi.nlm.nih.gov/pubmed/23364948.
65. Park SK, Park SK, Harlow SD, Zheng H, Karvonen-Gutierrez C, Thurston RC, Ruppert K, Janssen I, Randolph Jr JF (2017) Association between changes in oestradiol and follicle-stimulating hormone levels during the menopausal transition and risk of diabetes. *Diabet. Med.* **34** (4): 531-538. https://www.ncbi.nlm.nih.gov/pubmed/27973745.
66. LeBlanc ES, Kapphahn K, Hedlin H, Desai M, Parikh NI, Liu S, Parker DR, Anderson M, Aroda V, Sullivan S, Woods NF, Waring ME, Lewis CE, Stefanick M (2017) Reproductive history and risk of type 2 diabetes mellitus in postmenopausal women: findings from the Women's Health Initiative. *Menopause* **24** (1): 64-72. https://www.ncbi.nlm.nih.gov/pubmed/27465714.
67. Zidon TM, Padilla J, Fritsche KL, Welly RJ, McCabe LT, Stricklin OE, Frank A, Park Y, Clegg DJ, Lubahn DB, Kanaley JA, Vieira-Potter VJ (2020) Effects of ERbeta and ERalpha on OVX-induced changes in adiposity and insulin resistance. *J. Endocrinol.* **245** (1): 165-178. https://www.ncbi.nlm.nih.gov/pubmed/32053493.
68. Liu A, McLaughlin T, Liu T, Sherman A, Yee G, Abbasi F, Lamendola C, *et al*. (2009) Differential intra-abdominal adipose tissue profiling in obese, insulin-resistant women. *Obes Surg.* **19**: 1564-1573.
69. Tandon P, Wafer R, Minchin JEN. Adipose morphology and metabolic disease. *J. Exp. Biol*. **2018**: 221.
70. Imhoff BR, Hansen JM (2011) Differential redox potential profiles during adipogenesis and osteogenesis. *Cell Mol. Biol. Lett.* **16** (1): 149-161. https://www.ncbi.nlm.nih.gov/pubmed/21225471.
71. Masschelin PM, Cox AR, Chernis N, Hartig SM (2019) The impact of oxidative stress on adipose tissue energy balance. *Front. Physiol.* **10**: 1638. https://www.ncbi.nlm.nih.gov/pubmed/32038305.
72. Jarukamjorn K, Jearapong N, Pimson C, & Chatuphonprasert W (2016) A high-fat, high-fructose diet induces antioxidant imbalance and increases the risk and progression of nonalcoholic fatty liver disease in mice. *Scientifica (Cairo)* **2016**: 5029414. https://www.ncbi.nlm.nih.gov/pubmed/27019761.
73. Miller CG, Holmgren A, Arner ESJ, Schmidt EE (2018) NADPH-dependent and -independent disulfide reductase systems. *Free Radic. Biol. Med.* **127**: 248-261. https://www.ncbi.nlm.nih.gov/pubmed/29609022.
74. Wang X, Ma Y, Huang C, Wan Q, Li N, Bi Y (2008) Glucose-6-phosphate dehydrogenase plays a central role in modulating reduced glutathione levels in reed callus under salt stress. *Planta* **227** (3): 611-623. https://www.ncbi.nlm.nih.gov/pubmed/17952457.
75. Cui J, Shen Y, Li R (2013) Estrogen synthesis and signaling pathways during aging: from periphery to brain. *Trends Mol. Med.* **19** (3): 197-209. https://www.ncbi.nlm.nih.gov/pubmed/23348042
76. Iyengar NM, Hudis CA, Dannenberg AJ (2013) Obesity and inflammation: new insights into breast cancer development and progression. *Am. Soc. Clin. Oncol. Educ. Book* **33**: 46-51. https://www.ncbi.nlm.nih.gov/pubmed/23714453.

77. Bracht JR, Vieira-Potter VJ, De Souza Santos R, Oz OK, Palmer BF, Clegg DJ (2020) The role of estrogens in the adipose tissue milieu. *Ann. N. Y. Acad. Sci.* **1461** (1): 127-143. https://www.ncbi.nlm.nih.gov/pubmed/31868931.
78. Esposito E, Cuzzocrea S (2010) Antiinflammatory activity of melatonin in central nervous system. *Curr. Neuropharmacol.* **8** (3): 228-242. https://www.ncbi.nlm.nih.gov/pubmed/21358973.
79. Pandi-Perumal SR, Trakht I, Srinivasan V, Spence DW, Maestroni GJ, Zisapel N, Cardinali DP (2008) Physiological effects of melatonin: role of melatonin receptors and signal transduction pathways. *Prog. Neurobiol.* **85** (3): 335-353. https://www.ncbi.nlm.nih.gov/pubmed/18571301.
80. Reppert SM, Weaver DR, Ebisawa T (1994) Cloning and characterization of a mammalian melatonin receptor that mediates reproductive and circadian responses. *Neuron* **13** (5): 1177-1185. https://www.ncbi.nlm.nih.gov/pubmed/7946354.
81. Becker-Andre M, Wiesenberg I, Schaeren-Wiemers N, Andre E, Missbach M, Saurat JH, Carlberg C (1994) Pineal gland hormone melatonin binds and activates an orphan of the nuclear receptor superfamily. *J. Biol. Chem.* **269** (46): 28531-28534. https://www.ncbi.nlm.nih.gov/pubmed/7961794.
82. Benitez-King G, Huerto-Delgadillo L, & Anton-Tay F (1993) Binding of 3H-melatonin to calmodulin. *Life Sci.* **53** (3): 201-207. Https://www.ncbi.nlm.nih.gov/pubmed/8321083.
83. Ryu V, Zarebidaki E, Albers HE, Xue B, Bartness TJ (2018) Short photoperiod reverses obesity in Siberian hamsters via sympathetically induced lipolysis and browning in adipose tissue. *Physiol. Behav.* **190**: 11-20. https://www.ncbi.nlm.nih.gov/pubmed/28694154.
84. González A, Alvarez-García V, Martínez-Campa C, Alonso-González C, Cos S (2012) Melatonin promotes differentiation of 3T3-L1 fibroblasts. *J. Pineal Res.* **52** (1): 12-20. https://www.ncbi.nlm.nih.gov/pubmed/21718362.
85. Kato H, Tanaka G, Masuda S, Ogasawara J, Sakurai T, Kizaki T, Ohno H, Izawa T (2015) Melatonin promotes adipogenesis and mitochondrial biogenesis in 3T3-L1 preadipocytes. *J. Pineal Res.* **59** (2): 267-275. https://www.ncbi.nlm.nih.gov/pubmed/26123001.
86. Yang W, Tang K, Wang Y, Zhang Y, Zan L (2017) Melatonin promotes triacylglycerol accumulation via MT2 receptor during differentiation in bovine intramuscular preadipocytes. *Sci. Rep.* **7** (1): 15080. https://www.ncbi.nlm.nih.gov/pubmed/29118419.
87. Oliveira AC, Andreotti S, Sertie RAL, Campana AB, de Proença ARG, Vasconcelos RP, Oliveira KA, Coelho-de-Souza AN, Donato-Junior J, Lima FB (2018) Combined treatment with melatonin and insulin improves glycemic control, white adipose tissue metabolism and reproductive axis of diabetic male rats. *Life Sci.* **199**: 158-166. https://www.ncbi.nlm.nih.gov/pubmed/29501522.
88. Fernandez Vazquez G, Reiter RJ, Agil A (2018) Melatonin increases brown adipose tissue mass and function in Zucker diabetic fatty rats: implications for obesity control. *J. Pineal. Res.* **64** (4): e12472. https://www.ncbi.nlm.nih.gov/pubmed/29405372.
89. Agil A, Navarro-Alarcón M, Ruiz R, Abuhamadah S, El-Mir MY, Vázquez GF (2011) Beneficial effects of melatonin on obesity and lipid profile in young Zucker diabetic fatty rats. *J. Pineal Res.* **50** (2): 207-212. https://www.ncbi.nlm.nih.gov/pubmed/21087312.
90. Favero G, Stacchiotti A, Castrezzati S, Bonomini F, Albanese M, Rezzani R, Rodella LF (2015) Melatonin reduces obesity and restores adipokine patterns and metabolism in obese (ob/ob) mice. *Nutrit. Res.* **35** (10): 891-900. https://www.ncbi.nlm.nih.gov/pubmed/26250620.
91. Suriagandhi V, Nachiappan V (2022) Protective effects of melatonin against obesity-induced by leptin resistance. *Behav. Brain Res.* **417**: 113598. https://www.ncbi.nlm.nih.gov/pubmed/34563600.

92. Szewczyk-Golec K, Woźniak A, Reiter RJ (2015) Inter-relationships of the chronobiotic, melatonin, with leptin and adiponectin: implications for obesity. *J. Pineal Res.* **59** (3): 277-291. https://www.ncbi.nlm.nih.gov/pubmed/26103557.
93. Agil A, Reiter RJ, Jiménez-Aranda A, Ibán-Arias R, Navarro-Alarcón M, Marchal JA, Adem A, Fernández-Vázquez G (2013) Melatonin ameliorates low-grade inflammation and oxidative stress in young Zucker diabetic fatty rats. *J. Pineal Res.* **54** (4): 381-388. https://www.ncbi.nlm.nih.gov/pubmed/23020082.
94. Yin J, Li Y, Han H, Chen S, Gao J, Liu G, Wu X, Deng J, Yu Q, Huang X, Fang R, Li T, Reiter RJ, Zhang D, Zhu C, Zhu G, Ren W, Yin Y (2018) Melatonin reprogramming of gut microbiota improves lipid dysmetabolism in high-fat diet-fed mice. *J. Pineal Res.* **65** (4): e12524.
95. Wolden-Hanson T, Mitton DR, McCants RL, Yellon SM, Wilkinson CW, Matsumoto AM, Rasmussen DD (2000) Daily melatonin administration to middle-aged male rats suppresses body weight, intraabdominal adiposity, and plasma leptin and insulin independent of food intake and total body fat. *Endocrinol.* **141** (2): 487-497. https://www.ncbi.nlm.nih.gov/pubmed/30230594
96. Rios-Lugo MJ, Cano P, Jimenez-Ortega V, Fernandez-Mateos MP, Scacchi PA, Cardinali DP, Esquifino AI (2010) Melatonin effect on plasma adiponectin, leptin, insulin, glucose, triglycerides and cholesterol in normal and high fat-fed rats. *J. Pineal Res.* **49** (4): 342-348. https://www.ncbi.nlm.nih.gov/pubmed/20663045.
97. Terron MP, Delgado-Adamez J, Pariente JA, Barriga C, Paredes SD, Rodriguez AB (2013) Melatonin reduces body weight gain and increases nocturnal activity in male Wistar rats. *Physiol. Behav.* **118**: 8-13. https://www.ncbi.nlm.nih.gov/pubmed/23643827.
98. Mustonen AM, Nieminen P, Hyvarinen H (2002) Effects of continuous light and melatonin treatment on energy metabolism of the rat. *J. Endocrinol. Invest.* **25** (8): 7 16-723. 723 https://www.ncbi.nlm.nih.gov/pubmed/12240904.
99. Alonso-Vale MI, Andreotti S, Peres SB, Anhe GF, das Neves Borges-Silva C, Neto JC, Lima FB (2005) Melatonin enhances leptin expression by rat adipocytes in the presence of insulin. *Am. J. Physiol. Endocrinol. Metab.* **288** (4): E805-812. https://www.ncbi.nlm.nih.gov/pubmed/15572654.
100. Rasmussen DD, Mitton DR, Larsen SA, Yellon SM (2001) Aging-dependent changes in the effect of daily melatonin supplementation on rat metabolic and behavioral responses. *J. Pineal Res.* **31** (1): 89-94. https://www.ncbi.nlm.nih.gov/pubmed/11485011.
101. Liu K, Yu W, Wei W, Zhang X, Tian Y, Sherif M, Liu X, Dong C, Wu W, Zhang L, Chen J (2019) Melatonin reduces intramuscular fat deposition by promoting lipolysis and increasing mitochondrial function. *J. Lipid Res.* **60** (4): 767-782. https://www.ncbi.nlm.nih.gov/pubmed/30552289.
102. Thorp AA & Schlaich MP (2015) Relevance of sympathetic nervous system activation in obesity and metabolic syndrome. *J. Diabetes Res.* **2015**: 341583. https://www.ncbi.nlm.nih.gov/pubmed/26064978.
103. Demas GE, Bartness TJ (2001) Direct innervation of white fat and adrenal medullary catecholamines mediate photoperiodic changes in body fat. *Am. J. Physiol. Regul. Integr. Comp. Physiol.* **281** (5): R1499-1505. https://www.ncbi.nlm.nih.gov/pubmed/11641121.
104. Menéndez-Menéndez J, Martínez-Campa C (2018) Melatonin: An anti-tumor agent in hormone-dependent cancers. *Inter. J. Endocrinol.* **2018:** 3271948. https://www.ncbi.nlm.nih.gov/pubmed/30386380.
105. Veiga ECA, Simões R, Valenti VE, Cipolla-Neto J, Abreu LC, Barros EPM, Sorpreso ICE, Baracat MCP, Baracat EC, Soares Junior JM (2019) Repercussions of melatonin on the risk of breast cancer: a systematic review and meta-analysis. *Rev. Assoc. Med. Brasil.* **65** (5): 699-705. https://www.ncbi.nlm.nih.gov/pubmed/31166448.

106. Chottanapund S, Van Duursen MB, Navasumrit P, Hunsonti P, Timtavorn S, Ruchirawat M, Van den Berg M (2014) Anti-aromatase effect of resveratrol and melatonin on hormonal positive breast cancer cells co-cultured with breast adipose fibroblasts. *Toxicol. In Vitro* **7**: 1 215-1221. https://www.ncbi.nlm.nih.gov/pubmed/24929094.
107. Cipolla-Neto J, Amaral FG, Soares JM, Jr., Gallo CC, Furtado A, Cavaco JE, Gonçalves I, Santos CRA, Quintela T (2022) The Crosstalk between melatonin and sex steroid hormones. *Neuroendocrinol.* **112** (2): 1 15-129. https://www.ncbi.nlm.nih.gov/pubmed/33774638.
108. Otsuka F (2018) Interaction of melatonin and BMP-6 in ovarian steroidogenesis. *Vit. Horm.* **107**: 137-153. https://www.ncbi.nlm.nih.gov/pubmed/29544628.
109. Guan Q, Wang Z, Cao J, Dong Y, Chen Y (2021) Mechanisms of melatonin in obesity: A review. *Int. J. Mol. Sci.* **23** (1): 218. https://www.ncbi.nlm.nih.gov/pubmed/35008644.

Please cite this paper as:
Hermoso, D.A.M., Roza, L. da F., Hermoso, A.P.M., Klosowski, E.M., Moreno, F.N., Marçal Natali, M.R., Santos, T.C., Constantin, J., Constantin, R.P., Gilglione, E.H. and Ishii Iwamoto, E.L. 2024. Differential effects of melatonin on adipose tissues under normoestrogenic and estrogen-deficient conditions in rats. Melatonin Research. 7, 2 (Aug. 2024), 187-212. DOI:https://doi.org/https://doi.org/10.32794/mr112500175.